Robust stability optimization for linear delay systems in a probabilistic framework

Luca Fenzi, Wim Michiels

Department of Computer Science, KU Leuven, Belgium

Abstract

This paper is concerned with an eigenvalue based stabilization method for linear autonomous delay systems with uncertain parameters, modeled by a random vector. The dependence of the characteristic matrix on the uncertain parameters can be nonlinear; also delay values can be subject to uncertainty. Unlike the stability optimization methods for deterministic problems, which minimize the spectral abscissa, our approach shows better robust properties based on a more realistic model, where the uncertainty is taken into account by minimizing an objective function, consisting of the mean of the spectral abscissa with a variance penalty. The properties of the spectrum of delay differential algebraic equations of retarded type are analyzed and an integration method to compute the mean and variance of the spectral abscissa, which describes the stability property of the system, is presented. Subsequently the analysis of the behavior of the gradient of the characteristic roots is addressed, and a suitable explicit formula of the gradient of the objective function is presented. Finally, for designing the controller a suitable optimization routine, requiring the objective function and its gradient, is presented. The efficacy of the method is illustrated with numerical examples, including a model of an experimental heat-exchanger. The algorithms developed are publicly available.

Keywords: Eigenvalue analysis and optimization, delay differential algebraic equations of retarded type, uncertainty quantification, integrability of the spectral abscissa and its gradient.
2000 MSC: 65F15, 90C31, 60H35

Email addresses: Luca.Fenzi@cs.kuleuven.be (Luca Fenzi), Wim.Michiels@cs.kuleuven.be (Wim Michiels)

List of Acronyms

DDE	Delay Differential Equations
DDAE	Delay Differential Algebraic Equations
HANSO	Hybrid Algorithm for Non Smooth Optimization
BFGS	Broyden-Fletcher-Goldfarb-Shanno algorithm
QMC	Quasi Monte Carlos
SAE	Simple Active Eigenvalue
MSSAEs	Multiple (Semi)-Simple Active Eigenvalues
MNSSAEs	Multiple Non Semi-Simple Active Eigenvalues
p.d.f.	probability density function

1. Introduction

In the last decades, models involving delay have acquired more and more interest in different fields of science [1]. This trend is motived both by the studies on the established theory of delay differential equations (DDEs) [2, 3] and by the fact that the introduction of delay terms in a model can provide a better description of real phenomena.

Furthermore, in particular cases, the presence of delay may lead to stable systems, the so-called *stabilizing effect of delay*. Stabilization methods for linear time-delay has been widely studied [4, 5, 6] and applied in various engineering problems [7, 8, 9].

We study systems with feedback control, such that the plant has the following form:

$$\begin{cases} \dot{z}(t) = \sum_i F_i(\omega) z(t-\tau_i(\omega)) + \sum_i G_i(\omega) u(t-\tau_i(\omega)), \\ y(t) = \sum_i H_i(\omega) z(t-\tau_i(\omega)) + \sum_i L_i(\omega) u(t-\tau_i(\omega)), \end{cases} \tag{1}$$

where $\omega \in \mathbb{S} = [0,1]^D \subset \mathbb{R}^D$ models parameters subject to uncertainty, and $z(t)$, $u(t)$ and $y(t)$ are the state, the input, and the output at time t, respectively. Moreover the feedback controller can be either static or dynamic, in formula

Static
$$u(t) = \sum_i \hat{L}_i y(t - \tau_i(\omega)), \tag{2a}$$

Dynamic
$$\begin{cases} \dot{z_c}(t) = \sum_i \hat{F}_i z_c(t - \tau_i(\omega)) + \sum_i \hat{G}_i y(t - \tau_i(\omega)), \\ u(t) = \sum_i \hat{H}_i z_c(t - \tau_i(\omega)) + \sum_i \hat{L}_i y(t - \tau_i(\omega)). \end{cases} \tag{2b}$$

Since the novel approach deals with closed-loop delay systems of retarded type, we introduce the following assumption:

Assumption 1. *Either the plant or the controller is strictly proper, i.e. either L_i or $\hat{L}_i$ is zero for all i.*

For notational convenience, we recast (1) and (2) as a general Delay Differential Algebraic Equation (DDAE). Imposing $x = (z^{\mathrm{T}} y^{\mathrm{T}} z_c^{\mathrm{T}} u^{\mathrm{T}})^{\mathrm{T}} \in \mathbb{R}^n$ and $\mathbf{K} \in \mathbb{R}^k$ the vectorization of the control matrices $\hat{F}_i$, $\hat{G}_i$, $\hat{H}_i$, and $\hat{L}_i$, (1) and (2) can be rewritten as a DDAE with state $x(t)$ for $t > 0$

$$E\dot{x}(t) = \sum_{i=0}^{h} A_i(\omega, \mathbf{K}) x(t - \tau_i(\omega)), \tag{3}$$

where $\mathbf{K} \in \mathbb{R}^k$ parametrizes the controller, and E is a real matrix, whose dimension is $n \times n$ and rank e with $1 \leq e \leq n$.

Throughout the paper we make the following assumption:

Assumption 2. *For every $i \in \{0, \ldots, h\}$ the function $A_i : \mathbb{S} \times \mathbb{R}^k \to \mathbb{R}^{n \times n}$, $(\omega, \boldsymbol{K}) \mapsto A_i(\omega, \boldsymbol{K})$, and the function $\tau_i : \mathbb{S} \to \mathbb{R}_{\geq 0}$, $\omega \mapsto \tau_i(\omega)$, are smooth.*

For given $(\omega, \mathbf{K}) \in \mathbb{S} \times \mathbb{R}^k$, the stability properties of the trivial solution of (3), *i.e.* $x \equiv 0$, are determined by the non linear eigenvalue problem

$$\Lambda(\lambda) v = 0_{\mathbb{C}^n}, \text{ where } \Lambda(\lambda) = \lambda E - \sum_{i=0}^{h} A_i(\omega, \mathbf{K}) e^{-\lambda \tau_i(\omega)}. \tag{4}$$

It is important to point out that, by Assumption 1, the DDAE (3) arising from (1) and (2) is always of index 1 [10, 11, 12]. Furthermore, by the assumption, the eigenvalue problem (4) admits finitely many eigenvalues in any right half-plane.

The trivial solution of (1), (2), and (3) is asymptotically stable if the *spectral abscissa* $\alpha(\omega, \mathbf{K})$ is strictly negative, where the latter is defined by

$$\alpha(\omega, \mathbf{K}) = \max_{\lambda \in \mathbb{C}} \{\Re(\lambda) : \det(\Lambda(\lambda; \omega, \mathbf{K})) = 0\}, \tag{5}$$

where with the notation $\Lambda(\lambda; \omega, \mathbf{K})$ we stress the dependence on ω and $\mathbf{K}$ in the characteristic matrix (4). Therefore the spectral abscissa is the real part of the rightmost eigenvalue. On the latter, we need the following hypothesis, which is not restrictive from the application point of view:

Assumption 3. *For fixed $\boldsymbol{K}$ in $\mathbb{R}^k$ the rightmost eigenvalue is simple for almost all $\omega \in \mathbb{S}$, and for fixed $\omega \in \mathbb{S}$ the rightmost eigenvalue is simple for almost all $\boldsymbol{K} \in \mathbb{R}^k$.*

The research on stability optimization for delay free and time-delay systems focused, especially, on deterministic problems, *i.e.* the parameters of the system are assumed to be perfectly known [13, 14, 15]. These methods are interested in minimizing the objective function $\mathbf{K} \to \alpha(\tilde{\omega}, \mathbf{K})$ for $\tilde{\omega} \in \mathbb{S}$ fixed. However, the optimal solution of these methods might be sensitive w.r.t. small perturbation of the parameter (as we will see further on in Section 2). The stability optimization method can be robustified by minimizing the pseudospectral abscissa instead, which is, for the case of complex valued perturbations, connected with the $\mathcal{H}^\infty$ norm minimization problem. For computing the pseudospectral abscissa we refer to, *e.g.*, [16, 17, 18, 19, 20] and the references therein. The optimization of pseudospectral abscissa is included in the celebrated package HIFOO for fixed-order control design, see for instance [21]. The pseudospectra based approaches are well studied and powerful algorithms are available, with the most recent development focusing on algorithms for large-scale systems. In contrast to the presented approach, they are based on a worst-case analysis and they only exploit upper bounds on, usually, matrix valued uncertainty. Similarly, robustified stability measures, grounded in a $\mathcal{H}^2$ norm framework, have been proposed in [22] and in [23], in the context of periodic systems. Finally, methods from numerical bifurcation analysis, see *e.g.* [24], restrict to a small number of (controller or uncertain) parameters. For further extension see the book [4] and the reference therein.

In order to fully exploit the structure of the uncertainty and to take a probabilistic setting in the robustness analysis, we model the uncertainty on the parameters ω by means of the continuous real random vector $\boldsymbol{\omega}$ on the

probability space $(\Omega, \mathcal{F}, \mathcal{P})$ with probability density function $p_{\boldsymbol{\omega}}(\omega)$ defined on $\mathbb{S}$. In this context, the dimension D of the support of $\boldsymbol{\omega}$, *i.e.* $\mathbb{S}$, is the so-called *stochastic dimension* and it depends on the number of uncertain parameters of the model.

For the sake of simplicity, we make the following assumption:

Assumption 4. *The function $p_{\boldsymbol{\omega}} : \mathbb{S} \to [0, 1]$, $\omega \mapsto p_{\boldsymbol{\omega}}(\omega)$, is smooth.*

Remark 1. The Chebyshev Polynomial Chaos Expansion [25, 26] of the random vector $\boldsymbol{\omega}$ permits to restrict the support to $\mathbb{S} = [0, 1]^D$. Indeed, embedding the truncated Polynomial Chaos Expansion of $\boldsymbol{\omega}$ into the functions A_i and τ_i, the random vector, which model the uncertainty of system (1), (2), and (3), is uniformly distributed over the D-dimensional unit cube.

In order to take into account uncertainty in the stability optimization, our goal is to minimize a specific linear combination of the mean and the variance of the spectral abscissa, in formula

$$\min_{\mathbf{K} \in \mathbb{R}^k} f_{\text{obj}}(\mathbf{K}), \text{ with } f_{\text{obj}}(\mathbf{K}) = \mathbb{E}(\alpha(\boldsymbol{\omega}; \mathbf{K})) + c \cdot \text{Var}(\alpha(\boldsymbol{\omega}; \mathbf{K})), \tag{6}$$

where $c \in \mathbb{R}_{\geq 0}$ is a given trade off parameter, and $\mathbb{E}(\cdot)$ and $\text{Var}(\cdot)$ indicate respectively the mean and the variance.

We denote with bold Greek letters the random variables which models uncertainty, *e.g.* $\boldsymbol{\omega}$, while the normal font is used to indicate their realizations, $\omega \in \mathbb{S}$. In this view, for all $\mathbf{K} \in \mathbb{R}^k$, $\alpha(\boldsymbol{\omega}, \mathbf{K})$ is a random variable while $\alpha(\cdot, \mathbf{K}) : \mathbb{S} \to \mathbb{R}$, $\omega \mapsto \alpha(\omega, \mathbf{K})$ is a function w.r.t. the realization $\omega \in \mathbb{S}$. Analogous considerations hold for the eigenvalues λ.

As we shall see, the effects induced by the uncertain parameters and their respective optimization problems show that the proposed method has better robust stability properties than the solution of the corresponding deterministic stability optimization methods. Hence, the introduction of uncertainty in the parameters is not only motivated by search for more reliable models, but also to improve the robust properties of the solution. These aspects are anticipated in Section 2 and then developed in Section 5.

More in details, the structure of the paper is as follows. In Section 2, some motivation for taking into accounts uncertainty is given by illustrating a simple model of an oscillator with delayed feedback control and random parameters. Then, in Section 3 we examine the objective function for a fixed value of $\mathbf{K}$, studying the behavior of the spectral abscissa and approximating

the expectation and the variance in (6) with suitable integration methods. In Section 4, we analyze the optimization problem, computing the gradient of objective function (6) and studying the integrability of the gradient of the spectral abscissa. Hence, we outline the overall algorithm, based on approximation and minimization of objective function (6) handled by the Quasi Monte Carlo method and the software HANSO respectively. We end, in Section 5, with some numerical examples illustrating the applicability of the method to more general time-delay systems.

2. A motivating example: Oscillator with feedback delay

In order to motivate the proposed approach and illustrate important behaviors of the spectral abscissa, which we need in what follows, we consider an oscillator with input delay controlled by static state feedback:

$$\begin{cases} \dot{x}_1(t) = x_2(t), \\ \dot{x}_2(t) = -\nu^2 \cdot x_1(t) - 2\nu\xi \cdot x_2(t) + u(t-1), \\ u(t) = K_1 \cdot x_1(t) + K_2 \cdot x_2(t), \end{cases} \tag{7}$$

where x_1 is the normalized position, $x_2 = \dot{x}_1$ is the velocity, u is a force which acts with a delay $\tau = 1$, $\xi \in [0, 1]$ and $\nu > 0$ are respectively the damping ratio and the angular frequency (or natural frequency), and $\mathbf{K} = (K_1,\ K_2)^{\mathrm{T}}$ contains the control variables.

Without control, *i.e.* $\mathbf{K} = 0$, the eigenvalues of (7) are

$$\lambda_{1,2} = -\nu(\xi \pm \imath\sqrt{1-\xi^2}). \tag{8}$$

Hence the system without any control is stable, and in particular, is asymptotically stable for $\xi \in (0, 1]$. However the static delayed feedback control improves the stability and the robustness of the system.

We first consider the deterministic case where $\nu = 1$ and $\xi = 0.15$. Hence we apply the algorithm of [27] to find the optimal value $\mathbf{K}$ for which the spectral abscissa is minimal. Next, we take into account uncertainty on the damping ratio and angular frequency, where $\boldsymbol{\nu}$ and $\boldsymbol{\xi}$ are uniform and independent random variables in the intervals $[0.9, 1.1]$ and $[0.1, 0.2]$ respectively (in formula $\boldsymbol{\nu} \sim \mathcal{U}(0.9, 1.1)$, $\boldsymbol{\xi} \sim \mathcal{U}(0.1, 0.2)$). In the latter case, we optimize objective function (6), for different values of c.

Table 1: Numerical value of the spectral abscissa, its mean and variance for the optimized value of gain $\mathbf{K}$ (without control $\alpha((1, 0.15), 0) = -0.15$). The second column corresponds to optimizing the spectral abscissa for the deterministic model (7), while the third to the fifth columns show the results of optimizing (6) for different values of c.

	$\nu = 1$ $\xi = 0.15$	$\boldsymbol{\nu} \sim \mathcal{U}(0.9, 1.1),\ \boldsymbol{\xi} \sim \mathcal{U}(0.1, 0.2)$ $c = 0$	$c = 10$	$c = 100$
$\alpha((1, 0.15), \mathbf{K})$	-1.1387	-0.8473	-0.7823	-0.5811
$\mathbb{E}(\alpha(\boldsymbol{\omega}, \mathbf{K}))$	-0.6687	-0.7647	-0.7363	-0.5531
$\mathrm{Var}(\alpha(\boldsymbol{\omega}, \mathbf{K}))$	5.353e-2	1.572e-2	7.653e-3	1.829e-3

Table 1 shows the different results obtained fixing the optimal gain value $\mathbf{K}$ for the deterministic setting and for the system with uncertain parameters, varying c. The quantities under consideration are the spectral abscissa evaluated in $\nu = 1$ and $\xi = 0.15$, *i.e.* $\alpha((1, 0.15), \mathbf{K})$, the mean, $\mathbb{E}(\alpha(\boldsymbol{\omega}, \mathbf{K}))$, and the variance, $\mathrm{Var}(\alpha(\boldsymbol{\omega}, \mathbf{K}))$, where the random vector $\boldsymbol{\omega} = (\boldsymbol{\nu}, \boldsymbol{\xi})$ has independent components $\boldsymbol{\nu} \sim \mathcal{U}(0.9, 1.1)$ and $\boldsymbol{\xi} \sim \mathcal{U}(0.1, 0.2)$.

As shown in Table 1, the feedback control leads to a left shift of the

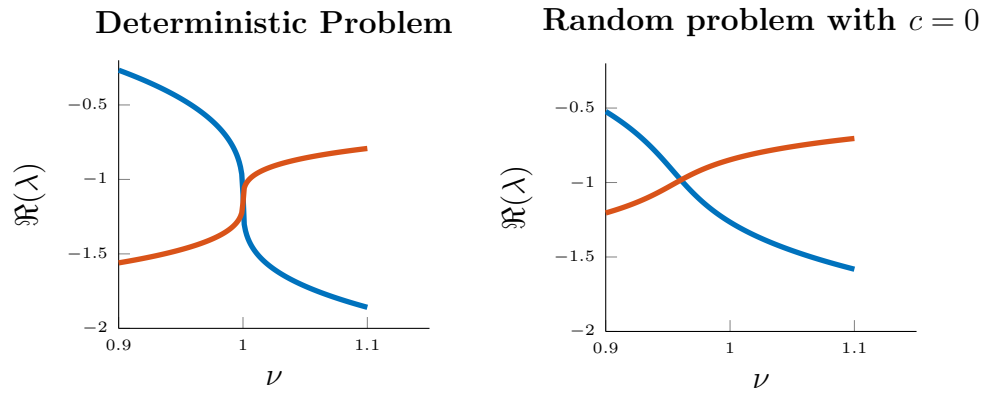

Figure 1: Bifurcation plots. The real parts of the rightmost eigenvalues are plotted as a function of ν over the interval $[0.9, 1.1]$ fixing $\xi = 0.15$. The left pane corresponds to gain values minimizing the spectral abscissa, the right pane to a minimum of (6) with $c = 0$.

spectral abscissa, improving the stability property of system (7) both in the deterministic and in the uncertain settings. The results in Table 1 and Figure 1 confirm the robustness of the method, taking into account uncertainty on the parameters. Even though for the deterministic problem we obtain a smaller value for the spectral abscissa $\alpha((1, 0.15), \mathbf{K})$ the expectation and the variance are bigger compared to the random problem. This result becomes even more evident if we look at the plots of the real parts of the rightmost eigenvalues, varying $\nu \in [0.9, 1.1]$ and fixing $\xi = 0.15$. Indeed a small perturbation of the parameters in the deterministic problem will widely increase the value of the spectral abscissa. The bifurcation plots of the uncertain problems, on the other hand, show a smoother behavior, guaranteeing better stability and robustness properties.

The behavior of the spectral abscissa, which can be inferred by Figure 1, is characterized by the multiplicity of the rightmost eigenvalues (we come to this in Section 3.1). Indeed the deterministic stability optimization leads in this example to a triple non semi-simple eigenvalue (Figure 3 *left*), and the spectral abscissa is not Lipschitz continuous in this point. On the contrary, solving the robust stability optimization problem leads to multiple simple eigenvalues (Figure 3 *right*), characterized by locally Lipschitz behavior of

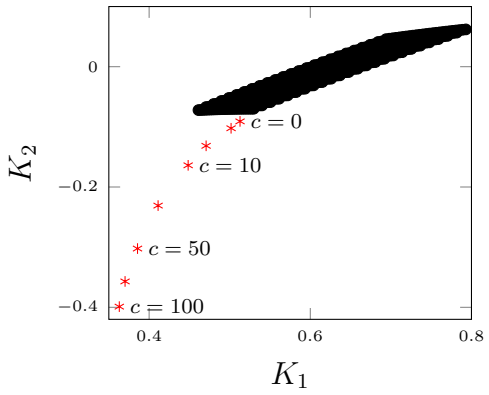

Figure 2: Globally optimal values of $\mathbf{K} = (K_1, K_2)^{\mathrm{T}}$ found with different methods. The black dots represent the optimal $\mathbf{K}$ when minimizing the spectral abscissa with parameters (ν, ξ) varying on a equally spaced grid of $[0.9, 1.1] \times [0.1, 0.2]$. The red asterisks represent the optimal values of $\mathbf{K}$ optimizing (6) with $c = 0, 1, 5, 10, 25, 50, 75, 100$.

the spectral abscissa.

Figure 2 shows that increasing the trade off parameter c, the optimal controller of the uncertain problem distances itself from the optimal gain values $\mathbf{K}$ obtained by the deterministic optimization problem of minimizing the spectral abscissa with parameters (ν, ξ) varying in a equally spaced grid of $[0.9, 1.1] \times [0.1, 0.2]$.

3. Evaluation of the objective function

In order to evaluate objective function (6) for a fixed $\mathbf{K}$, we need to evaluate integrals over the whole uncertainty domain $\mathbb{S}$, taking into account the lack of smoothness properties of the integrand. Indeed, as illustrated in Figure 1, the spectral abscissa is, in general, not everywhere differentiable, even not everywhere Lipschitz continuous in $\mathbb{S}$, and moreover, the points in $\mathbb{S}$, where the spectral abscissa presents a non smooth behavior, are not known a priori.

The purpose of this Section is twofold: it furnishes the preliminaries on the optimization problem and it illustrates the post-processor method to analyze the optimal solution, *i.e.* to study the problem for fixed control parameters.

First of all, we prove that objective function (6) exists, which is essentially stated in the following proposition.

Proposition 1. *Under Assumptions 1 - 4, the mean and the variance of the spectral abscissa exist, and they can be expressed as*

$$\begin{aligned} \mathbb{E}(\alpha(\boldsymbol{\omega}, \boldsymbol{K})) &= \int_{\mathbb{S}} \alpha(\omega, \boldsymbol{K}) p_{\boldsymbol{\omega}}(\omega) \, \mathrm{d}\omega, \\ \mathrm{Var}(\alpha(\boldsymbol{\omega}, \boldsymbol{K})) &= \int_{\mathbb{S}} \left(\alpha(\omega, \boldsymbol{K}) - \mathbb{E}(\alpha(\boldsymbol{\omega}, \boldsymbol{K}))\right)^2 p_{\boldsymbol{\omega}}(\omega) \, \mathrm{d}\omega. \end{aligned} \tag{9}$$

Proof. For fixed $\mathbf{K} \in \mathbb{R}^k$, by Assumption 2 the spectral abscissa $\alpha(\cdot, \mathbf{K})$ is a continuous function on $\mathbb{S}$; integrals (9) exist, since the integrands are continuous functions (Assumption 4) and the domain of integration is a compact subset of $\mathbb{R}^D$ ($\mathbb{S} = [0, 1]^D$).

3.1. Behavior of the spectral abscissa

The spectral abscissa essentially behaves as the rightmost eigenvalue, which is smooth *a.e.* in $\mathbb{S} \times \mathbb{R}^k$, by Assumption 3. However, as already

shown in Figure 1, the spectral abscissa is in general not everywhere smooth, and this is due to the presence of the maximum operator in (5) and it is also due to the behavior of multiple rightmost eigenvalues. Indeed, in a set of measure zero, there can be more than one rightmost eigenvalue (counted with the multiplicity) with the same real part, and in these points the spectral abscissa is not differentiable [15]. We distinguish the different qualitative behaviors using the following definition:

Definition 1. An *active eigenvalue* is a characteristic root which satisfies $\Re(\lambda) = \alpha(\omega, \mathbf{K})$ and $\Im(\lambda) \geq 0$.

Simple Active Eigenvalue (SAE) For all $\omega \in \mathbb{S}$ there exists only one active eigenvalue with algebraic multiplicity 1, *i.e.* the rightmost eigenvalue is simple.

When the active eigenvalue is simple, which is the general behavior by Assumption 3, the spectral abscissa is analytic. In this case, the following proposition states an explicit formula to evaluate the partial derivative of the active eigenvalue w.r.t. a component of $\mathbf{K}$ (for a proof refer to Lemma 2.7 in [28]).

Proposition 2. *Assume that for* $(\omega, \boldsymbol{K}) \in \mathbb{S} \times \mathbb{R}^k$ *the rightmost eigenvalue* $\lambda(\omega, \boldsymbol{K})$ *is simple and let* $v, u \in \mathbb{C}^n$ *denote the right and left eigenvector, respectively. Then the relation*

$$\frac{\partial \lambda(\omega, \boldsymbol{K})}{\partial K_j} = \frac{-u^* \frac{\partial \Lambda(\lambda)}{\partial K_j} v}{u^* \frac{\partial \Lambda(\lambda)}{\partial \lambda} v}, \text{ for } j = 1, \ldots, k, \tag{10}$$

holds, where $\Lambda(\lambda)$ *is the matrix defined in* (4)*, and* u^* *is the conjugate transpose of* u*.*

Thanks to the proposition, the partial derivative of the spectral abscissa w.r.t. K_j for $j = 1, \ldots, k$ can be recast as

$$\frac{\partial \alpha(\omega, \mathbf{K})}{\partial K_j} = \Re \left(\frac{-u(\omega, \mathbf{K})^* \frac{\partial \Lambda(\lambda)}{\partial K_j} v(\omega, \mathbf{K})}{u(\omega, \mathbf{K})^* \frac{\partial \Lambda(\lambda)}{\partial \lambda} v(\omega, \mathbf{K})} \right), \quad (\omega, \mathbf{K}) \text{ a.e. in } \mathbb{S} \times \mathbb{R}^k. \tag{11}$$

Moreover, using the definition of characteristic matrix (4), we can express the partial derivative of $\Lambda(\lambda)$ w.r.t. K_j and λ in (11) and (10) as

$$\frac{\partial \Lambda(\lambda)}{\partial K_j} = -\sum_{i=0}^{h} \frac{\partial A_i(\omega, \mathbf{K})}{\partial K_j} e^{-\lambda \tau_i(\omega)}, \quad \frac{\partial \Lambda(\lambda)}{\partial \lambda} = E + \sum_{i=0}^{h} \tau_i(\omega) A_i(\omega, \mathbf{K}) e^{-\lambda \tau_i(\omega)}. \tag{12}$$

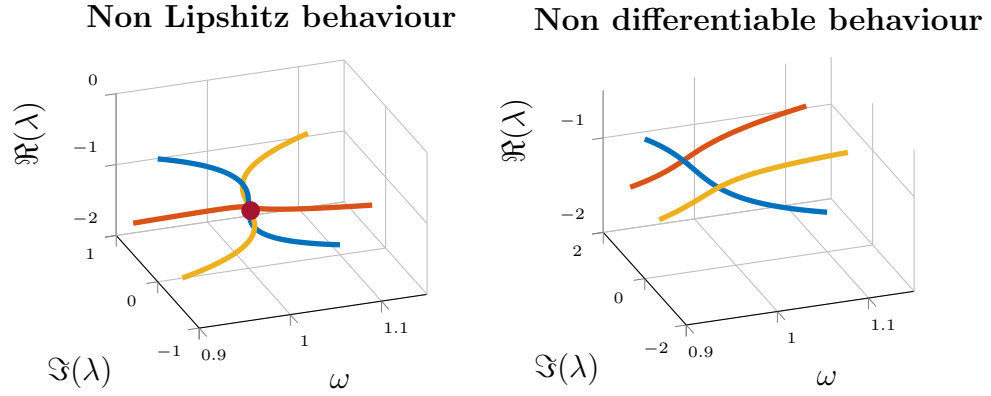

Figure 3: The real and imaginary parts of the rightmost eigenvalues of the system (7) are plotted against $\omega \in [0.9, 1.1]$ fixing $\xi = 0.15$; the left pane corresponds to a minimum of the spectral abscissa and illustrates the MNSSAEs case, while the right pane is evaluated in a minimum of (6) with $c = 0$ and it exhibits a MSSAEs case.

Multiple (Semi)-Simple Active Eigenvalues (MSSAEs) In the domain $\mathbb{S}$, the active eigenvalue is simple, except in a set of measure zero where the rightmost eigenvalues are multiple but simple or semi-simple. In this case, the active eigenvalues are crossing but not overlapping each other (Figure 3 *right*) or, if they overlap, the algebraic multiplicity coincides with the geometric one. In this situation the spectral abscissa is, in general, not differentiable but it is still locally Lipschitz continuous on $\mathbb{S}$ (Figure 1 *right*).

Multiple Non Semi-Simple Active Eigenvalues In the domain $\mathbb{S}$ there are points where the active eigenvalue has algebraic multiplicity larger than the geometric one (Figure 3 *left*). In this case the spectral abscissa is typically not even Lipschitz continuous (see the left pane of Figure 1 for the splitting of a triple non semi-simple eigenvalue).

Throughout the paper, we will often refer to the SAE, MSSAEs and MNSSAEs cases characterizing the behaviors of the spectral abscissa. Moreover the system (7) with uncertain parameters ($\boldsymbol{\nu} \sim \mathcal{U}(0.9, 1.1)$ and $\boldsymbol{\xi} \sim \mathcal{U}(0.1, 0.2)$) will be taken as prototype for the different tests in the theoretical sections (Figures 4, and 5). Table 2 reviews the gain values of the system, previously described, for whom the spectral abscissa behaves according to the three different cases: SAE, MSSAEs and MNSSAEs.

Table 2: Numerical values of the control parameters $\mathbf{K} = (K_1, K_2)^{\mathrm{T}}$ for the system (7) with uncertain parameters $\boldsymbol{\nu} \sim \mathcal{U}(0.9, 1.1)$ and $\boldsymbol{\xi} \sim \mathcal{U}(0.1, 0.2)$, corresponding to different behaviors of the spectral abscissa on $\mathbb{S}$ (SAE, MSSAEs, and MNSSAEs).

	SAE	MSSAEs	MNSSAEs
K_1	0.2	0.5105	0.6179
K_2	0.2	-0.0918	-0.0072

3.2. Approximation of the objective function for a fixed $\boldsymbol{K}$

The computation of objective function (6) is based on approximating integrals (9). As shown in Section 3.1, the integrands of (9) exhibit a continuous non differentiable behavior, which affects the convergence rate of the evaluation of the objective function.

In our implementation, the numerical integration is accomplished by the Quasi Monte Carlo (QMC) methods [29, 30, 31]. The QMC integration relies on low-discrepancy (or quasi-random) sequences, that improve the convergence rate of the standard Monte Carlo method based on random and pseudo-random sequences. QMC integration loses its effectiveness if the integrand is not smooth, however it is almost always as accurate as the Monte Carlo method [31]. As suggested by [30], we construct a set $\Xi = \{u^i\}_{i=1}^M$ of M quasi-random points uniformly distributed in the D-dimensional unit cube, using the Halton sequences up to stochastic dimension $D = 6$, and the Sobol sequences for higher stochastic dimensions. For every $u^i \in \Xi$, evaluating the spectral abscissa $\alpha(u^i)$ of (1), (2), and (3) with $\omega = u^i$, we can approximate

integrals (9), *i.e.* the mean and variance of $\alpha(\boldsymbol{\omega})$, using the following formula:

$$\mathbb{E}(\alpha(\boldsymbol{\omega})) \approx \overline{\alpha(u^i)p_{\boldsymbol{\omega}}(u^i)}, \ \mathrm{Var}(\alpha(\boldsymbol{\omega})) \approx \frac{1}{M}\sum_{i=1}^{M}\left(\alpha(u^i) - \overline{\alpha(u^i)p_{\boldsymbol{\omega}}(u^i)}\right)^2 p_{\boldsymbol{\omega}}(u^i), \tag{13}$$

where $\overline{\alpha(u^i)p_{\boldsymbol{\omega}}(u^i)}$ indicate the arithmetic average of $\{\alpha(u^i)p_{\boldsymbol{\omega}}(u^i)\}_{i=1}^{M}$.

In order to compute an approximation of the spectral abscissa, we consider the deterministic systems (1), (2), and (3), where $\omega = u^i \in \Xi$ is fixed. Following the approach of [27], an active eigenvalue is first approximated by the Infinitesimal Generator Approach [32, 3] and then corrected by applying Newton's method to (4). The realization $\alpha(u^i)$ of $\alpha(\boldsymbol{\omega})$ is, hence, evaluated taking the real part of the corrected rightmost eigenvalue.

We conclude this section, recalling prototype system (7) with uncertain parameters. We evaluate the convergence rate w.r.t. the number of samples M for the mean and the variance of the spectral abscissa in the different cases SAE, MSSAEs, MNSSAEs. Figure 4 shows $\mathcal{O}\left(M^{-1}\right)$ convergence rate is reached to approximate integrals (9). These results show that QMC integration converges faster than the standard Monte Carlo method, which has $\mathcal{O}\left(M^{-\frac{1}{2}}\right)$ convergence rate (see [31, 29] for more details).

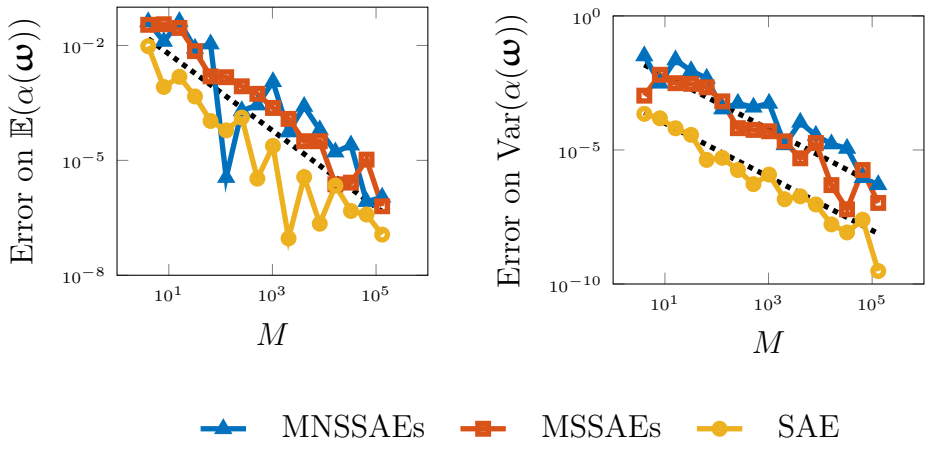

Figure 4: Errors to evaluate integrals (9) with QMC methods for different behaviors of the spectral abscissa. The black dotted lines indicate a convergence rate of $\mathcal{O}\left(M^{-1}\right)$. The numerical problem is summarized in Table 2.

4. The optimization problem

This section is devoted to the major features of the robust stabilization problem. First we characterize and compute the gradient of the objective function. Hence, in Section 4.1 we deal with the integrability of the gradient of the spectral abscissa $\nabla_{\mathbf{K}}\alpha(\omega, \mathbf{K})$, which plays a fundamental role to prove the existence of the gradient of the objective function $\nabla_{\mathbf{K}} f(\mathbf{K})$. In Section 4.2 we approximate $\nabla_{\mathbf{K}} f(\mathbf{K})$ using QMC integration and we show the convergence rate of this approximation. At the end, in Section 4.3, a suitable method to handle the optimization problem (6) is proposed.

Likewise to the notational comment in Section 1, we denote with

$$(\omega, \mathbf{K}) \mapsto \nabla_{\mathbf{K}}\alpha(\omega, \mathbf{K}) \text{ and } (\omega, \mathbf{K}) \mapsto \alpha(\omega, \mathbf{K})\nabla_{\mathbf{K}}\alpha(\omega, \mathbf{K}), \tag{14}$$

two real functions defined on $\mathbb{S}\times\mathbb{R}^k$, while $\nabla_{\mathbf{K}}\alpha(\boldsymbol{\omega}, \mathbf{K})$ and $\alpha(\boldsymbol{\omega}, \mathbf{K})\nabla_{\mathbf{K}}\alpha(\boldsymbol{\omega}, \mathbf{K})$ are continuous real random vectors.

Since we are dealing with a minimization problem, the gradient of the objective function can be used as a search direction for the optimization. The following proposition provides a formula to evaluate the gradient of the objective function using the gradient of the spectral abscissa.

Proposition 3. *If the gradient of the spectral abscissa w.r.t. the control parameters $\boldsymbol{K}$ is an integrable function on $\mathbb{S}$, then the gradient of objective function* (6) *exists and it can be expressed by*

$$\nabla_{\boldsymbol{K}} f_{obj}(\boldsymbol{K}) = [1-2c\mathbb{E}(\alpha(\boldsymbol{\omega}, \boldsymbol{K}))]\mathbb{E}(\nabla_{\boldsymbol{K}}\alpha(\boldsymbol{\omega}, \boldsymbol{K}))+2c\mathbb{E}(\alpha(\boldsymbol{\omega}, \boldsymbol{K})\nabla_{\boldsymbol{K}}\alpha(\boldsymbol{\omega}, \boldsymbol{K})). \tag{15}$$

Proof. The objective function is a linear combination of integrals (9); therefore its gradient w.r.t. $\mathbf{K}$ is the gradient of the linear combination of these integrals. In Section 3 we proved that $\alpha(\omega, \mathbf{K})$ is integrable over $\mathbb{S}$. Providing that $\nabla_{\mathbf{K}}\alpha(\omega, \mathbf{K})$ is also integrable over $\mathbb{S}$, we can differentiate the integrals using the result obtained in [33]. Hence, we evaluate the gradient w.r.t. $\mathbf{K}$ of the mean and the variance

$$\begin{aligned}
\nabla_{\mathbf{K}}\mathbb{E}(\alpha(\boldsymbol{\omega}, \mathbf{K})) &= \mathbb{E}(\nabla_{\mathbf{K}}\alpha(\boldsymbol{\omega}, \mathbf{K})) \text{ a.e. on } \mathbb{S},\\
\nabla_{\mathbf{K}} \operatorname{Var}(\alpha(\boldsymbol{\omega}, \mathbf{K})) &= \int_{\mathbb{S}} 2\left(\alpha(\omega, \mathbf{K}) - \mathbb{E}(\alpha(\boldsymbol{\omega}, \mathbf{K}))\right) \nabla_{\mathbf{K}}\left(\alpha(\omega, \mathbf{K}) - \mathbb{E}(\alpha(\boldsymbol{\omega}, \mathbf{K}))\right) p_{\boldsymbol{\omega}}(\omega)\,\mathrm{d}\omega\\
&= 2\mathbb{E}(\alpha(\boldsymbol{\omega}, \mathbf{K})\nabla_{\mathbf{K}}\alpha(\boldsymbol{\omega}, \mathbf{K})) - 2\mathbb{E}(\alpha(\boldsymbol{\omega}, \mathbf{K}))\mathbb{E}(\nabla_{\mathbf{K}}\alpha(\boldsymbol{\omega}, \mathbf{K})) \text{ a.e. on } \mathbb{S}.
\end{aligned}$$

The gradient of the objective function is well defined and can be expressed by (15).

4.1. Differentiability of the objective function

Let us analyze the assumption of Proposition 3. We first demonstrate the integrability of the gradient of the spectral abscissa when the control parameters $\mathbf{K}$ are affected by uncertainty as well. Next we prove, under a Lipschitz condition on the spectral abscissa, that its gradient is integrable. Moreover, we show a case-study where the latter result is extended to a less restrictive setting.

4.1.1. A particular case: the control parameters are uncertain

Let the length of the vector $\mathbf{K}$ be less or equal to the stochastic dimension, *i.e.* $k \leq D$. The following proposition states that if all control parameters in $\mathbf{K}$ are affected by uncertainty then the hypothesis of Proposition 3 is satisfied.

Proposition 4. *Let the components of $\boldsymbol{\omega}$ be recast as $\boldsymbol{\omega} = (\tilde{\boldsymbol{\omega}}, \hat{\boldsymbol{\omega}})$, where $\tilde{\boldsymbol{\omega}}$ and $\hat{\boldsymbol{\omega}}$ are random vectors with $D-k$ and k components respectively. For $i = 1, \ldots, k$, if $\hat{\omega}_i$ occurs only in the coefficients of the matrices $\{A_j\}_{j=1}^h$ of system (1), (2), and (3), where K_i occurs, and assume that these coefficients can be recast as functions of $K_i + \hat{\omega}_i$ and $\tilde{\omega}$, then function $\omega \mapsto \nabla_{\boldsymbol{K}} \alpha(\omega, \boldsymbol{K})$ is an integrable function on $\mathbb{S}$, for all $\boldsymbol{K} \in \mathbb{R}^k$.*

Proof. Under the conditions of the proposition, $\alpha(\omega, \mathbf{K}) = \beta(\tilde{\omega}, \mathbf{K} + \hat{\omega})$ for some continuous function β.

In the SAE case, the spectral abscissa is differentiable and we can apply the chain rule to its partial derivative w.r.t. K_i

$$\frac{\partial \beta(\tilde{\omega}, \mathbf{K} + \hat{\omega})}{\partial K_i} = \frac{\partial \beta(\tilde{\omega}, \mathbf{K} + \hat{\omega})}{\partial \hat{\omega}_i}, \quad \forall i = 1, \ldots, k. \tag{16}$$

Clearly this continuous function is integrable over the compact set $\mathbb{S}$.

In the MSSAEs case, the partial derivative of the spectral abscissa exhibits a discontinuity in a set of measure zero, but it is of bounded variation on $\mathbb{S}$. Hence, it is easy to prove that is integrable also in this case.

In the MNSSAEs case, we consider the partial derivative of the spectral abscissa w.r.t. K_i, for all $i = 1, \ldots, k$ and we stress only the $\hat{\omega}_i$-dependency in the eigenvalues. The effects of the uncertainty on K_i can be seen as a real linear perturbation on some coefficients of the matrices which describe the system. Let $\lambda(\hat{\omega}_i^0)$ be an isolated active eigenvalue with partial multiplicity $(\ell_1, \ldots, \ell_l)$. Then in a neighborhood of $\hat{\omega}_i^0$, $\mathcal{S}$, the spectrum of $\Lambda(\lambda)$ presents

$\mathcal{L} = \ell_1 + \ldots + \ell_l$ eigenvalues $\lambda_s(\hat{\omega}_i)$, $s = 1, \ldots, \mathcal{L}$ (counted with multiplicity) such that, by the Weierstrass Preparation theorem, $\lambda_s(\hat{\omega}_i)$ are algebraic functions of $\hat{\omega}_i$ and can be represented by branches of Puiseux series

$$\mu_t(\hat{\omega}_i) = \lambda(\hat{\omega}_i^0) + c_t(\hat{\omega}_i - \hat{\omega}_i^0)^{\frac{1}{q_t}} + \mathcal{O}\left((\hat{\omega}_i - \hat{\omega}_i^0)^{\frac{2}{q_t}}\right),\ t = 1, \ldots, \mathcal{M},\ \hat{\omega}_i \in \mathcal{S}, \tag{17}$$

where $c_t \in \mathbb{C}$, $q_t \in \mathbb{N}$, $q_1 \geq \ldots \geq q_{\mathcal{M}}$ and $q_1 + \ldots + q_{\mathcal{M}} = \mathcal{L}$ [34].

In $\mathcal{S} \setminus \{\hat{\omega}_i^0\}$, applying (16), the partial derivative of the spectral abscissa w.r.t. K_i behaves as $\Re\left(\frac{\partial \mu_t(\hat{\omega}_i)}{\partial \hat{\omega}_i}\right)$ for some $t \in \{1, \ldots, \mathcal{M}\}$, which are integrable on $\mathcal{S}$. Without loss of generality $\mathcal{S}$ is contained in the $\hat{\omega}_i$-projection of $\mathbb{S}$, and hence $\frac{\partial \alpha(\omega, \mathbf{K})}{\partial K_i}$ is integrable for all $i = 1, \ldots, k$.

Systems, which satisfy the assumptions of Proposition 4, take into account uncertainty on the implemented feedback control in the optimization problem. Referring to the motivating example (Equation (7)), we would satisfy the conditions of Proposition 4 if the uncertainty would not be on the system's parameters ν and ξ, but on the controller parameters K_1 and K_2. It should be said that in applications, the accuracy of the feedback control is usually high in view of the uncertainty on the other parameters of the system.

4.1.2. General case

In the previous case, summarized in Proposition 4, we were differentiating $\alpha(\omega, \mathbf{K})$ w.r.t to the variable ω on whom we were integrating, applying (16). In the more general setting, however, we are differentiating w.r.t. $\mathbf{K}$ and we are integrating over the variable ω on $\mathbb{S}$. In this context the following theorem states that, under a Lipschitz condition, $\nabla_{\mathbf{K}} \alpha(\omega, \mathbf{K})$ is integrable on $\mathbb{S}$.

Theorem 1. *If for some $L > 0$, the function $\alpha(\omega, \cdot) : \mathbb{R}^k \to \mathbb{R}$, $\boldsymbol{K} \mapsto \alpha(\omega, \boldsymbol{K})$ is locally Lipschitz in $\boldsymbol{K}$ at $\boldsymbol{K} = \boldsymbol{K}_0$, with Lipschitz constant L, for all $\omega \in \mathbb{S}$, then the gradient of the spectral abscissa is integrable on $\mathbb{S}$ at $\boldsymbol{K} = \boldsymbol{K}_0$, and, consequently, $\nabla_{\boldsymbol{K}} f_{obj}(\boldsymbol{K})$ exists at $\boldsymbol{K} = \boldsymbol{K}_0$.*

Proof. Let $U \subset \mathbb{R}^k$ denote the neighborhood of $\mathbf{K}_0$ such that $\alpha(\omega, \cdot)$ restricted to U is Lipschitz continuous for all $\omega \in \mathbb{S}$. In order to obtain the thesis, we need to prove that $\frac{\partial \alpha(\omega, \mathbf{K}_0)}{\partial K_j}$ is integrable on $\mathbb{S}$, for $j = 1, \ldots, k$ and then apply Proposition 3. Denoting e_j the jth column vector of the identity

matrix $I_k \in \mathbb{R}^{k\times k}$, for all $h \in \mathbb{R}$ such that $\mathbf{K}_0 + he_j \in U$, for the Lipschitz continuity, we have

$$|\alpha(\omega, \mathbf{K}_0 + he_j) - \alpha(\omega, \mathbf{K}_0)| \leq L|h|, \quad \forall \omega \in \mathbb{S}. \tag{18}$$

By Assumption 3 the spectral abscissa is *a.e.* differentiable on $\mathbb{S}$, hence, we obtain

$$\left|\frac{\partial \alpha(\omega, \mathbf{K}_0)}{\partial K_j}\right| = \lim_{h\to 0} \frac{|\alpha(\omega, \mathbf{K}_0 + he_j) - \alpha(\omega, \mathbf{K}_0)|}{|h|} \leq L, \qquad \textit{a.e.} \text{ in } \mathbb{S}. \tag{19}$$

Since $\frac{\partial \alpha(\omega, \mathbf{K}_0)}{\partial K_j}$ exists *a.e.* on the compact set $\mathbb{S}$ and is bounded on $\mathbb{S}$, we arrive at the assertion.

We remind that the spectral abscissa is locally Lipschitz in both ω and $\mathbf{K}$ (and hence Theorem 1 holds) when the active eigenvalues are (semi)-simple, *i.e.* in the SAE and MSSAEs cases. However we were not able to prove in the MNSSAEs case that the gradient of the objective function (15) always exists under Assumptions 1 - 4, even though we have strong indication that this property holds, as motivated by the following case-study.

Example 1. *Let us consider a delay system with stochastic dimension* $D = 1$ *and* $\mathbb{S} = [-1, 1]$, *such that for* $\omega = 0$ *the rightmost eigenvalue* λ_0 *has algebraic multiplicity* $m > 1$ *and geometric multiplicity equal to* 1. *Assume moreover that the Complete Regular Splitting (CRS) property holds for* $\omega = 0$, *i.e.* $u_0^* \frac{\partial \Lambda(\lambda_0)}{\partial \omega} v_0 \neq 0$, *where* u_0 *and* v_0 *are the left and the right eigenvector corresponding to* λ_0, *respectively.*

By Assumption 3 there exists an open interval (a, b) *with* $a < 0 < b$ *where the eigenvalue* $\lambda(\omega)$ *is isolated, except for* $\omega = 0$. *If we restrict to the interval* $(0, b)$, $\lambda(\omega)$ *and its right and left eigenvectors,* $v(\omega)$ *and* $u(\omega)$ *respectively, admit a Puiseux expansion at* 0 *[35], in formula*

$$\lambda(\omega) = \lambda_0 + \sum_{i=1}^{\infty} \omega^{\frac{i}{m}} \lambda_i,$$

$$v(\omega) = v_0 + \sum_{i=1}^{\infty} \omega^{\frac{i}{m}} v_i, \quad u(\omega) = u_0 + \sum_{i=1}^{\infty} \omega^{\frac{i}{m}} u_i.$$

Moreover, the partial derivative w.r.t. λ of the characteristic matrix, $\frac{\partial \Lambda(\lambda;\omega,\boldsymbol{K})}{\partial \lambda}$, can be expressed with a Taylor expansion in increasing powers of $\omega^{\frac{i}{m}}$, exploiting the Puiseux series of $\lambda(\omega)$, obtaining

$$\frac{\partial \Lambda(\lambda;\omega,\boldsymbol{K})}{\partial \lambda} = \frac{\partial \Lambda(\lambda_0;0,\boldsymbol{K})}{\partial \lambda} + \frac{\partial^2 \Lambda(\lambda_0;0,\boldsymbol{K})}{\partial \lambda^2}\lambda_1 \omega^{\frac{1}{m}} + \mathcal{O}\left(\omega^{\frac{2}{m}}\right). \tag{20}$$

By Assumption 2, $\Lambda(\lambda;\omega,\boldsymbol{K})$ behaves smoothly w.r.t. $\boldsymbol{K}$ and then $\frac{\partial \Lambda(\lambda;\omega,\boldsymbol{K})}{\partial K_j}$ is bounded for all $j = 1,\dots,k$; as a consequence $u(\omega)^* \frac{\partial \Lambda(\lambda;\omega,\boldsymbol{K})}{\partial K_j} v(\omega)$ is bounded since u_0 and v_0 are well defined and finite. In addition, since λ_0 is not semi-simple, we have that $u_0^* \frac{\partial \Lambda(\lambda_0;0,\boldsymbol{K}))}{\partial \lambda} v_0 = 0$. Hence, formula (10) suggests the following behavior for the derivative of the rightmost eigenvalues w.r.t. K_j for $j = 1,\dots,k$ as a function of $\omega \in (0,b)$:

$$\frac{\partial \lambda(\omega)}{\partial K_j} = \frac{-u(\omega)^* \frac{\partial \Lambda(\lambda;\omega,\boldsymbol{K})}{\partial K_j} v(\omega)}{\omega^{\frac{1}{m}}\left(u_1^* \frac{\partial \Lambda(\lambda_0;0,\boldsymbol{K})}{\partial \lambda} v_0 + u_0^* \frac{\partial^2 \Lambda(\lambda_0;0,\boldsymbol{K})}{\partial \lambda^2}\lambda_1 v_0 + u_0^* \frac{\partial \Lambda(\lambda_0;0,\boldsymbol{K})}{\partial \lambda} v_1\right) + \mathcal{O}\left(\omega^{\frac{2}{m}}\right)}.$$

Hence, $\frac{\partial \alpha(\omega,\boldsymbol{K})}{\partial K_j}$ behaves as $\omega^{-\frac{1}{m}}$ in $(0,b)$, if

$$u_1^* \frac{\partial \Lambda(\lambda_0;0,\boldsymbol{K})}{\partial \lambda} v_0 + u_0^* \frac{\partial^2 \Lambda(\lambda_0;0,\boldsymbol{K})}{\partial \lambda^2}\lambda_1 v_0 + u_0^* \frac{\partial \Lambda(\lambda_0;0,\boldsymbol{K})}{\partial \lambda} v_1 \neq 0. \tag{21}$$

Analogous result holds in the interval $(a,0)$, providing that the gradient of the spectral abscissa w.r.t. $\boldsymbol{K}$ is integrable in a neighborhood of $\omega = 0$; hence, for Proposition 3, the gradient of the objective function (15) exists.

4.2. Computation of the gradient of the objective function

We can compute the gradient of the objective function, $\nabla_{\mathbf{K}} f_{\text{obj}}$, with relations (11), (12), and (15). From a computational point of view, we compute the spectral abscissa at only a finite number of points where we can expect $\alpha(\omega,\mathbf{K})$ to be differentiable. Hence, fixing a set $\Xi = \{u^i\}_{i=1}^M$ of M realizations of $\boldsymbol{\omega}$, we approximate the integrals in (15) through the QMC integration:

$$\begin{aligned}\nabla_{\mathbf{K}} f_{\text{obj}}(\mathbf{K}) \approx & [1 - 2c\overline{\alpha(u^i,\mathbf{K}) p_{\boldsymbol{\omega}}(u^i)}]\overline{\nabla_{\mathbf{K}} \alpha(u^i,\mathbf{K}) p_{\boldsymbol{\omega}}(u^i)} + \\ & + 2c\overline{\alpha(u^i,\mathbf{K}) \nabla_{\mathbf{K}} \alpha(u^i,\mathbf{K}) p_{\boldsymbol{\omega}}(u^i)}.\end{aligned}$$

The partial derivative of the spectral abscissa is, under milder conditions, integrable over $\mathbb{S}$, but in the MNSSAE case it might not be square integrable

(setting $m = 2$ in Example 1, then $\frac{\partial \alpha(\omega, \mathbf{K})}{\partial K_j}$ behaves as $\omega^{-\frac{1}{2}}$, under mild condition). The latter is a difficult case (*e.g.*, note that there is no theoretical convergence bound for the Monte Carlo method to evaluate (15), since the integrand is not mean square integrable [31]). However, numerical experiments, see *e.g.*, Figure 5, show that QMC integration has a convergence rate of $\mathcal{O}(M^{-\frac{1}{2}})$, which is the usual convergence rate of the Monte Carlo method; also in the MSSAEs case we obtain a $\mathcal{O}(M^{-\frac{1}{2}})$ convergence rate, due to the discontinuities of the partial derivative of the spectral abscissa. In the SAE case, it is possible to evaluate the gradient of the objective function, $\nabla_{\mathbf{K}} f_{\text{obj}}(\mathbf{K})$, with the QMC with an accuracy of $\mathcal{O}(M^{-1})$, which is an improvement w.r.t. the Monte Carlo method.

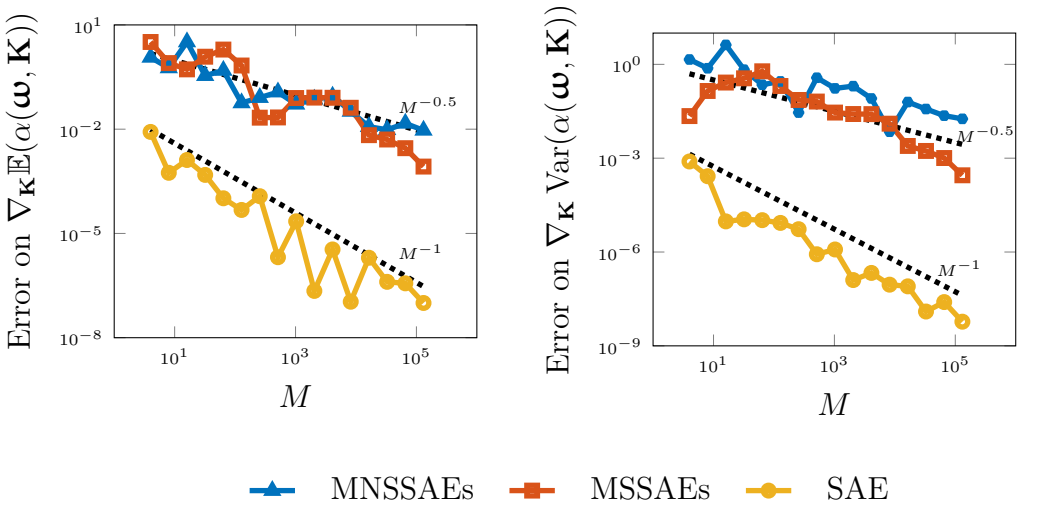

Figure 5: Euclidean norm of the errors on $\nabla_{\mathbf{K}} \mathbb{E}(\alpha(\boldsymbol{\omega}, \mathbf{K}))$ and $\nabla_{\mathbf{K}} \operatorname{Var}(\alpha(\boldsymbol{\omega}, \mathbf{K}))$ approximated via QMC methods for different behaviors of the spectral abscissa, *i.e.*, the gradients of the quantities analyzed in Figure 4. Note that (15) can be recast as $\nabla_{\mathbf{K}} \mathbb{E}(\alpha(\boldsymbol{\omega}, \mathbf{K})) + c \nabla_{\mathbf{K}} \operatorname{Var}(\alpha(\boldsymbol{\omega}, \mathbf{K}))$. The black dotted lines indicate the convergence rate. The numerical problem is summarized in Table 2.

4.3. Solving the optimization problem

A first important property of the objective function (6), regarding its optimization, is that it is non-convex and hence may have many local minima. Indeed the non-convexity of the optimization of the spectral abscissa,

illustrated in [15], are carried over from the deterministic to the stochastic problem.

Moreover, by Assumption 3, we are theoretically dealing with an objective function which is everywhere differentiable under mild assumptions, obtaining hence a smoother optimization problem than the deterministic spectral abscissa optimization problem. However the QMC methods, which approximate integrals (9) through the formula (13), lead to a non smooth objective function, which is more regular than the spectral abscissa but presents further local minima, as illustrated in Example 2 and in the right pane of Figure 6. This is because by the discretization of the integral, its smoothing effect is lost.

Example 2. *Consider the system*

$$x''(t) = -\omega^2 x(t) + \boldsymbol{K}\omega^2 x(t-1), \tag{22}$$

where ω *is a realization of* $\boldsymbol{\omega} \sim \mathcal{U}(0.9, 1.1)$ *and* $\boldsymbol{K}$ *is varying in* $[0.6, 0.85]$.

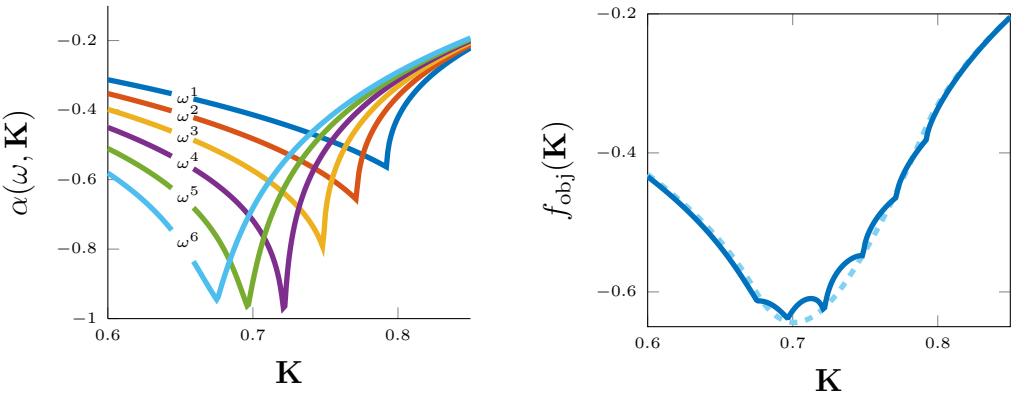

Figure 6: (*Left* pane) Spectral abscissa of system (22) versus $\mathbf{K}$ for nominal value of the random parameter $\omega^i = 0.9 + 0.04 \cdot i$ for $i = 0, \ldots, 5$. (*Right* pane) Comparison between the exact objective function with $c = 0$ (dashed line) and its approximation computed on the sample $\{\omega^i\}_{i=0}^5$ (solid line).

The left pane of Figure 6 shows the spectral abscissa as a function of $\boldsymbol{K} \in [0.6, 0.85]$ *fixing* $\omega^i = 0.9 + 0.04 \cdot i$ *for* $i = 0, \ldots, 5$. *These functions are used to compute the approximation of the objective function* (6) *with*

$c = 0$ *(Figure 6 right, solid line), which is compared with the exact mean of the spectral abscissa (Figure 6 right, dashed line). As we can observe, the objective function is differentiable for all* $\boldsymbol{K} \in [0.6, 0.85]$ *while its numerical approximation on* $\{\omega^i\}_{i=0}^5$ *presents non differentiable points whenever one of the spectral abscissa* $\alpha(\omega^i, \boldsymbol{K})$ *is non Lipschitz continuous. However, the approximated* $f_{obj}(\boldsymbol{K})$ *is more regular than the associated spectral abscissas. Indeed, the non smooth behaviors of* $\alpha(\omega^i, \boldsymbol{K})$ *at* $\boldsymbol{K} = \hat{\boldsymbol{K}}_i$ *is averaged with the smoothed spectral abscissa functions* $\alpha(\omega^j, \boldsymbol{K})$ $j \neq i$.

It is important to note that this example stresses a pessimistic non locally Lipschitz behaviors of the (discretized) objective function. Indeed, the robust optimization (6) *usually drives the iterations away from the MNSSAE case. Moreover, we expect a smoother behavior, similar to the theoretical one, increasing the number of sample points.*

The properties of the optimization problem requires optimization software which can deal with non-convex and non smooth unconstrained minimization. For this reason we use the MATLAB code HANSO (Hybrid Algorithm for Non Smooth Optimization) [13], which merges the Gradient Sampling and BFGS methods requiring the objective function and its gradient w.r.t. the control parameters $\mathbf{K}$, whenever the latter is differentiable.

However, an accurate computation of f_{obj} and $\nabla_{\mathbf{K}} f_{\text{obj}}$ is computationally demanding. Therefore, we focus on a deterministic description of the random parameters $\boldsymbol{\omega}$, fixing a set $\Xi_{\text{opt}} = \{u^i\}_{i=1}^{M_{\text{opt}}}$ of M_{opt} realizations in $\mathbb{S}$, *i.e.* the D-dimensional unit cube, as explained in Section 3.2. Hence, the objective function and its gradient are always computed on Ξ_{opt} by the optimization method, in such a way that the fluctuations of the realizations of $\boldsymbol{\omega}$ will not effect the accuracy of the solver and in order to reduce the computational time of the overall algorithm.

Remark 2. Based on experiments, the termination tolerance of the BFGS phase is set equal to the convergence rate of the QMC method in the SAE case, empirically evaluated as M_{opt}^{-1} in Figure 5; while the Gradient Sampling ends when the evaluation distance for gradients is less than $M_{\text{opt}}^{-0.5}$, the convergence rate in the MSSAE and MNSSAE cases, Figure 5.

After the evaluation of the optimal gain value $\mathbf{K}$ through HANSO, which is initialized by default on 10 random starting vectors for the BFGS phase, it is convenient to do a post-processor analysis of the solution using M_{post} realizations of $\boldsymbol{\omega}$, as explained in Section 3, where $M_{\text{opt}} \ll M_{\text{post}}$.

If the norm of the gradient of the objective function, evaluated in the post-processor analysis, *i.e.* $\|\nabla_{\mathbf{K}} f_{\text{obj}}\|$, is approximately zero, then the accuracy M_{opt}, used to compute the optimal gain value, is enough to obtain reliable solutions; otherwise we refine the sample Ξ_{opt} and we run HANSO again, initialized with the optimal gain value $\mathbf{K}$ obtained with the previous rough grid. Indeed, the optimization software might stop in a local minimum, which arises from the discretization of the objective function on the sample Ξ_{opt}, *e.g.* see the right pane of Figure 6; a refinement of the grid, in this case, might hence reveal a better optimal gain value.

To give an overview of the method, we provide a sketch of the overall algorithm implemented.

Algorithm 1.

Optimization Problem

1. *Construct a set of M_{opt} realizations of $\boldsymbol{\omega}$, i.e. Ξ_{opt}, using the Halton sequences up to stochastic dimension $D = 6$, and the Sobol sequences for higher stochastic dimensions.*
2. *Via the HANSO code, find the optimal gain value for* (1), (2), *and* (3), *giving as inputs the approximations of the objective function and its gradient on Ξ_{opt}.*

Post-Processor Analysis

3. *Likewise step 1, construct a set of M_{post} realizations of $\boldsymbol{\omega}$, i.e. Ξ_{post}.*
4. *Approximate f_{obj} and $\nabla_{\boldsymbol{K}} f_{obj}$ on Ξ_{post}.*

if $\|\nabla_{\boldsymbol{K}} f_{obj}\| \approx 0$ ***then***

return $\boldsymbol{K}$, $\mathbb{E}(\alpha(\boldsymbol{\omega}; \boldsymbol{K}))$, *and* $\text{Var}(\alpha(\boldsymbol{\omega}; \boldsymbol{K}))$.

else

Increase M_{opt} and repeat starting from step 1, initializing HANSO with the optimal gain value previously found.

5. Numerical Examples

We illustrate the new approach analyzing three case-studies. A user-friendly MATLAB implementation of the proposed method, with the examples and test, here exposed, is publicly available [36].

5.1. Static and Dynamic controllers

As a first example, we consider the prototype system [27] with stochastic dimension $D = 3$, expressed in the form (1)

$$\begin{cases} \dot{z}(t) = A(\omega)z(t) + Bu(t - \tau(\omega)), \\ y(t) = z(t), \end{cases} \tag{23}$$

where

$$A(\boldsymbol{\omega}) = \begin{pmatrix} \boldsymbol{\omega}_2 & -0.03 & 0.2 \\ \boldsymbol{\omega}_3 & -0.04 & -0.005 \\ -0.06 & 0.2 & -0.07 \end{pmatrix}, \; B = \begin{pmatrix} -0.1 \\ -0.2 \\ 0.1 \end{pmatrix}, \quad \begin{array}{c} \tau(\boldsymbol{\omega}) = \boldsymbol{\omega}_1 \sim \mathcal{U}(4.9, 5.1), \\ \boldsymbol{\omega}_2 \sim \mathcal{U}(-0.09, -0.07), \\ \boldsymbol{\omega}_3 \sim \mathcal{U}(0.15, 0.25). \end{array}$$

As shown in Figure 7 (left pane), the p.d.f. of the spectral abscissa with $\mathbf{K} = 0$, *i.e.* $\alpha(\boldsymbol{\omega}, 0)$, is contained in the positive real line, ensuring the instability of the system. We design a dynamic controller of the form (2)

$$\begin{cases} \dot{z}_c(t) = \hat{F}z_c(t) + \hat{G}y(t), \quad z_c(t) \in \mathbb{R}^{n_c}, \\ u(t) = \hat{H}z_c(t) + \hat{L}y(t), \quad u(t) \in \mathbb{R}, \end{cases} \tag{24}$$

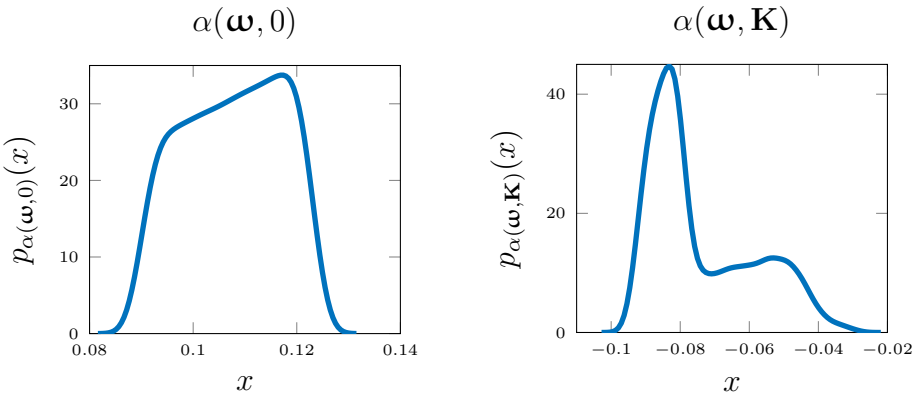

Figure 7: Probability density function of the spectral abscissa $\alpha(\boldsymbol{\omega}, \mathbf{K})$ for system (23) without control, *i.e.* $\mathbf{K} = 0$, (left pane) and when objective function (6) is minimal for $n_c = 0$ $c = 0$ (right pane).

where $\mathbf{K}$ is the vectorization of the control matrices $\hat{F}$, $\hat{G}$, $\hat{H}$, and $\hat{L}$, as already shown in the transformation from (1) and (2) to (3).

We apply the optimization approach to objective function (6) considering $c = 0,\ 10^3$ on the system with static control, $n_c = 0$ and with dynamic feedback, $n_c = 1,\ 2$. The results, obtained with $M_{\text{opt}} = 10^3$ and $M_{\text{post}} = 10^4$, are shown in Table 3.

Designing a controller with higher order n_c will lead us to a small value of the mean of the spectral abscissa. Even though, as shown in Figure 7 (*right pane*), the resulting support of the spectral abscissa minimizing (6) with static feedback control is already contained in the negative real line, ensuring asymptotic stability properties for the system (23).

Table 3: Comparison between system (23) without control and the results of minimizing objective function (6) with different controls of the form (24).

	Without control	Static Control		Dynamic Control			
	$\mathbf{K} = 0$	$n_c = 0$		$n_c = 1$		$n_c = 2$	
		$c = 0$	$c = 10^3$	$c = 0$	$c = 10^3$	$c = 0$	$c = 10^3$
$\alpha(\bar{\boldsymbol{\omega}}, \mathbf{K})$	0.10806	-0.089548	-0.056152	-0.16200	-0.11570	-0.22318e	-0.17037
$\mathbb{E}(\alpha(\boldsymbol{\omega}, \mathbf{K}))$	0.1076	-0.0739	-0.0551	-0.1195	-0.1133	-0.19950	-0.17049
$\text{Var}(\alpha(\boldsymbol{\omega}, \mathbf{K}))$	9.1770e-05	2.3655e-04	8.6305e-06	6.9411e-04	1.1774e-05	1.0074e-03	1.2609e-05

5.2. Stabilization problem with distributed delay

As a second example, we consider a plant with a distributed delay term

$$\dot{x}(t) = A_1 x(t) + B(\omega)u(t - \tau_1) + A_2 x(t - \tau_2(\omega)) + \int_{t-\tau_2(\omega)}^{t} A_3 x(\theta)\, \mathrm{d}\theta, \quad (25)$$

where

$$A_1 = \begin{pmatrix} 0.1 & 0 & 0 \\ 0.2 & 0 & -0.2 \\ 0.3 & 0.1 & -0.2 \end{pmatrix}, \quad A_2 = \begin{pmatrix} -0.2 & 0 & 0 \\ -0.4 & -0.2 & 0.4 \\ -0.4 & -0.1 & 0.2 \end{pmatrix},$$

$$A_3 = \begin{pmatrix} 0.1 & -0.2 & 0 \\ 0 & 0.1 & 0.1 \\ -0.1 & 0 & 0.1 \end{pmatrix}, \ B(\boldsymbol{\omega}) = \begin{pmatrix} \boldsymbol{\omega}_2 \\ 0 \\ 0 \end{pmatrix}, \quad \begin{array}{c} \tau_1 = 1, \\ \tau_2(\boldsymbol{\omega}) = \boldsymbol{\omega}_1 \sim \mathcal{U}(5.9, 6.1), \\ \boldsymbol{\omega}_2 \sim \mathcal{U}(0.075, 0.125), \end{array}$$

with a static feedback control: $u(t) = \mathbf{K}^{\mathrm{T}} x(t)$. Note that for fixed τ_2 and ω_2, the system is analyzed in [14]. Setting $h(t)$ equal to the distributed delay term of (25), and differentiating $h(t)$, the system (25) can be recast as

$$\begin{cases} \dot{x}(t) = A_1 x(t) + B(\omega) u(t - \tau_1) + A_2 x(t - \tau_2(\omega)) + h(t), \\ \dot{h}(t) = A_3 x(t) - A_3 x(t - \tau_2(\omega)). \end{cases} \tag{26}$$

Imposing $z = (x^{\mathrm{T}} \dot{h}^{\mathrm{T}} u^{\mathrm{T}})^{\mathrm{T}}$, system (26) with static feedback can be rewritten as a DDAE (3)

$$\dot{z}(t) = \begin{pmatrix} A_1 & I & 0 \\ A_3 & 0 & 0 \\ K^{\mathrm{T}} & 0 & -1 \end{pmatrix} z(t) + \begin{pmatrix} 0 & 0 & B(\omega) \\ 0 & 0 & 0 \\ 0 & 0 & 0 \end{pmatrix} z(t - \tau_1) + \begin{pmatrix} A_2 & 0 & 0 \\ -A_3 & 0 & 0 \\ 0 & 0 & 0 \end{pmatrix} z(t - \tau_2(\omega)). \tag{27}$$

Formulations (25) and (26) are almost equivalent; however, the dimension of the latter system is double w.r.t. the dimension of (25). As a consequence of differentiating function $h(t)$, (26) has 3 additional non-physical zero eigenvalues w.r.t. the spectrum of (25). These additional zero eigenvalues, which appear also in the formulation (27), can be removed and the results obtained minimizing objective function (6) with $c = 0, 10, 10^2, 10^3$ using $M_{\mathrm{opt}} = 10^3$, $M_{\mathrm{post}} = 10^4$, are shown in Table 4.

Table 4: Results of minimizing the objective function (6) for the DDAE (27).

	$c = 0$	$c = 10$	$c = 10^2$	$c = 10^3$
$\alpha(\bar{\boldsymbol{\omega}}, \mathbf{K})$	0.16312	0.16275	0.16942	0.23747
$\mathbb{E}(\alpha(\boldsymbol{\omega}, \mathbf{K}))$	0.1845	0.1846	0.1866	0.2375
$\mathrm{Var}(\alpha(\boldsymbol{\omega}, \mathbf{K}))$	2.2629e-04	2.0903e-04	1.6418e-04	7.0138e-06

5.3. Heating System

The optimization method has been tested on the linear model of the experimental heat transfer set up, described in [37], which was tested also with deterministic methods [38, 27].

The mathematical model consists of 10 delay differential equations, which involves six different delays in the state and two different delays in the inputs

$$\dot{x}(t) = \sum_{i=0}^{5} A_i(\omega, \mathbf{K}) x(t-\tau_i) + B_1 u(t-\tau_5) + B_2 u(t-\tau_6), \quad x(t) \in \mathbb{R}^{10}, \tag{28}$$

see [38] for the corresponding matrices and delay values.

We consider system (28) with static feedback control: $u(t) = \mathbf{K}^{\mathrm{T}} x(t)$. First, we apply the deterministic stability optimization [27]. Hence we apply the proposed method setting an uncertainty of 10% on the nominal value of the temperature of the left cooler, denoted by T_{LC} in [37], and moreover setting an uncertainty of 10% on the nominal temperatures of both coolers, denoted by T_{LC} and T_{RC} in [37]. The temperatures of both coolers depends on the seasonal temperature of the outdoor air, hence they may vary in the following range:

$$\boldsymbol{T}_{LC} \sim \mathcal{U}(13.5, 16.5), \quad \boldsymbol{T}_{RC} \sim \mathcal{U}(15.3, 18.7). \tag{29}$$

The uncertainty on $\boldsymbol{T}_{LC}$ affects the $(10,10)$th entry of matrix A_0, the $(10,9)$th entry of A_2, and the only non-zero coefficient (10th entry) of vector B_1. On the other hand, the uncertainty on $\boldsymbol{T}_{RC}$ affects the $(6,6)$th entry of matrix A_0, and the $(6,5)$th entry of A_2.

To obtain the results shown in Table 5, we set $c = 0$, 10, 10^2, 10^3 and we firstly run Algorithm 1 using a number of samples $M_{\mathrm{opt}} = 500$ and $M_{\mathrm{post}} = 10^3$. However, the results did not always satisfy the following relations:

$$\mathbb{E}(\alpha(\boldsymbol{\omega}, \mathbf{K}_1)) \geq \mathbb{E}(\alpha(\boldsymbol{\omega}, \mathbf{K}_2), \quad \mathrm{Var}(\alpha(\boldsymbol{\omega}, \mathbf{K}_1)) \leq \mathrm{Var}(\alpha(\boldsymbol{\omega}, \mathbf{K}_2), \tag{30}$$

where $\mathbf{K}_1$ and $\mathbf{K}_2$ are the optimal controller with objective functions (6) with $0 \leq c_1 < c_2$, due to the presence of local minima that are not global. Hence, for each value of c, we re-run Algorithm 1 initializing HANSO on all optimal gain values previously found and refining the set of realizations using $M_{\mathrm{opt}} = 10^3$ and $M_{\mathrm{post}} = 10^4$. The latter results, shown in Table 5, satisfies criterion (30) and the gradient of the objective function, evaluated in the post-processor analysis, is approximatively zero.

[1]The solutions obtained with $c = 10$ and $c = 10^2$ are similar to the one corresponding to $c = 0$, for this reason we do not report them.

Table 5: Numerical value of the spectral abscissa, its mean and variance w.r.t. the uncertainty on T_{LC} and the uncertainties on T_{LC} and T_{RC} for the optimized value of gain $\mathbf{K}$. The second column corresponds to optimizing the spectral abscissa for the deterministic case, while the third to the sixth columns show the results of optimizing (6) for $c = 0,\ 10^3$ and imposing different uncertainties. The variables, which are considered as random, and the control gain are typed in bold face.[1]

	$T_{LC} = 15$ $T_{RC} = 17$	$\boldsymbol{T}_{LC} \sim \mathcal{U}(13.5, 16.5)$ $T_{RC} = 17$		$\boldsymbol{T}_{LC} \sim \mathcal{U}(13.5, 16.5)$ $\boldsymbol{T}_{RC} \sim \mathcal{U}(15.3, 18.7)$	
		$c = 0$	$c = 10^3$	$c = 0$	$c = 10^3$
$\alpha((T_{LC}, T_{RC}), \mathbf{K})$	-0.0641408	-0.0634016	-0.0633525	-0.0634057	-0.06314255
$\mathbb{E}(\alpha((\boldsymbol{T}_{LC}, T_{RC}), \mathbf{K}))$	-0.0626683	-0.0633310	-0.0633273	-0.0632089	-0.0630809
$\mathrm{Var}(\alpha((\boldsymbol{T}_{LC}, T_{RC}), \mathbf{K}))$	2.6465e-06	4.9526e-08	1.0437e-08	2.7837e-07	8.2656e-08
$\mathbb{E}(\alpha((\boldsymbol{T}_{LC}, \boldsymbol{T}_{RC}), \mathbf{K}))$	0.05990348	-0.05411337	-0.0577562	-0.0629809	-0.0629191
$\mathrm{Var}(\alpha((\boldsymbol{T}_{LC}, \boldsymbol{T}_{RC}), \mathbf{K}))$	8.4117e-06	1.4040e-05	1.4668e-05	2.8111e-07	1.0105e-07

Table 5 shows how the uncertainty on the parameters may affect the optimal gain values and, consequently, the momenta of the spectral abscissa. Indeed, increasing the stochastic dimension may lead to different optimal gain controllers. It is important to notice that the deterministic solution may lead to unstable system if the temperatures of both coolers are affected by uncertainty, since the mean value is contained in the positive real line.

6. Concluding Remarks

We present a novel stability optimization method for linear interconnected systems with time delays affected by uncertainty, which are modeled by DDAEs of retarded type where some coefficients are determined by the realizations of a random vector. The novel approach has several advantages. First, the system description (3) allows to model a wide class of interconnected systems, with no restriction on the number of constant and distributed delays, with the possibilities to design static and dynamic feedback controllers. Second, all coefficients of the DDAE system, including the delays, can be effected by uncertainty, *i.e.*, they can be described by random variables with a given probability density function. Uncertainty does not only lead to more realistic system but permits to achieve a more robust solution compared to the associated deterministic design. Third, the solu-

tions are more reliable and suitable for realistic applications. As shown in the last numerical example in Section 5.3, small perturbations on some parameters, may render stable solutions in the deterministic setting unstable. Considering the novel approach, however, the solution can be stabilized and robustified also in this latter case. The approach has been implemented in generic software which is publicly available [36].

The presented approach is complementary to the approaches grounded in the pseudospectral abscissa optimization. First, while the former adopts a probabilistic setting in describing the uncertainty and in the robust stability criterion, the latter takes a worst-case setting, using only upper bounds on the uncertainty. Second, in the pseudospectra setting typically matrix valued perturbations are considered, hence, many parameters are subject to uncertainty. Very efficient algorithms have become available meanwhile but it remains difficult to take into account a given structure of the uncertainty, in particular if the dependence of the characteristic matrix on an uncertain parameters is nonlinear (*e.g.*, an uncertain delay). In applications this issue, combined with the worst-case treatment, may lead to an over bounding on the actual uncertainty and a safe but conservative design. On the contrary, with the adopted approach the parametric dependence and structure of the uncertainty can be easily taken into account, but from a computational view, only a small number of uncertain parameters can be considered, following from the multivariate integrals involving eigenvalue functions that are not always smooth. This is the currently main limitation of the approach. It should be said, however, that the overall approach concerns an off-line controller design.

In the light of this discussion, further investigations will mainly focus on the refinement of the novel approach to larger scale problem with higher stochastic dimension, providing a fast solver and an accurate analysis of the computational complexity of the algorithm. Other search-directions will address the analysis between the solutions and the uncertain parameters, the study of the Pareto front varying weight parameter c, and the improvements for the sampling algorithm and for the optimization software.

Acknowledgments

Special thanks goes to Tomáš Vyhlídal, Paul McGahan, and Dan Pilbauer for their constructive comments on the heating system and on the codes.

This work has been supported by the Program of Interuniversity Attraction Poles of the Belgian Federal Science Policy Office (IAP P6-DYSCO), by OPTEC, the Optimization in Engineering Center of the KU Leuven, by the project G.0712.11N of the Research Foundation- Flanders (FWO - Vlaanderen), and by the project UCoCoS, funded by the European Unions Horizon 2020 research and innovation program under the Marie Skodowska-Curie Grant Agreement No 675080.

References

[1] T. Erneux, Applied Delay Differential Equations, Springer, New York, 2008.

[2] J. K. Hale, S. M., V. Lunel, Introduction to Functional Differential Equations, Springer, New York, 2013.

[3] D. Breda, S. Maset, R. Vermiglio, Stability of Linear Delay Differential Equations, Springer, New York, 2014.

[4] W. Michiels, S.-I. Niculescu, Stability, Control, and Computation for Time-Delay Systems, SIAM, 2015.

[5] R. Sipahi, T. Vyhlídal, S. I. Niculescu, P. Pepe (Eds.), Time Delay Systems: Methods, Applications and New Trends, Springer-Verlag, Berlin Heidelberg, 2012.

[6] J. J. Loiseau, W. Michiels, S. I. Niculescu, R. Sipahi (Eds.), Topics in Time Delay Systems, Springer-Verlag, Berlin Heidelberg, 2009.

[7] T. Vyhlídal, N. Olgac, V. Kučera, Delayed resonator with acceleration feedback – complete stability analysis by spectral methods and vibration absorber design, J. Sound. Vib. 333 (25) (2014) 6781–6795. doi:10.1016/j.jsv.2014.08.002.

[8] T. Vyhlídal, M. Hromčík, Parameterization of input shapers with delays of various distribution, Automatica 59 (2015) 256–263. doi:10.1016/j.automatica.2015.06.025.

[9] M. Diehl, K. Mombaur (Eds.), Fast Motions in Biomechanics and Robotics, Springer, Berlin Heidelberg, 2006.

[10] S. Gumussoy, W. Michiels, Fixed-order h-infinity control for interconnected systems using delay differential algebraic equations, SIAM J. Control Optim. 49 (5) (2011) 2212–2238. doi:10.1137/100816444.

[11] N. H. Du, V. H. Linh, V. Mehrmann, D. D. Thuan, Stability and robust stability of linear time-invariant delay differential-algebraic equations, SIAM J. Matrix Anal. & Appl. 34 (4) (2013) 1631–1654. doi:10.1137/130926110.

[12] S. L. Campbell, Singular linear systems of differential equations with delays, Applicable Analysis 11 (2) (1980) 129–136. doi:10.1080/00036818008839326.

[13] M. L. Overton, Stability optimization for polynomials and matrices, in: Spectral Analysis, Stability and Bifurcations, Wiley-Blackwell, 2014, pp. 351–375.

[14] W. Michiels, K. Engelborghs, P. Vansevenant, D. Roose, Continuous pole placement for delay equations, Automatica 38 (5) (2002) 747–761. doi:10.1016/s0005-1098(01)00257-6.

[15] J. Vanbiervliet, K. Verheyden, W. Michiels, S. Vandewalle, A nonsmooth optimisation approach for the stabilisation of time-delay systems, ESAIM: COCV 14 (3) (2007) 478–493. doi:10.1051/cocv:2007060.

[16] M. W. Rostami, New algorithms for computing the real structured pseudospectral abscissa and the real stability radius of large and sparse matrices, SIAM J. Sci. Comput. 37 (5) (2015) 447–471. doi:10.1137/140975413.

[17] W. Michiels, N. Guglielmi, An iterative method for computing the pseudospectral abscissa for a class of nonlinear eigenvalue problems, SIAM J. Sci. Comput. 34 (4) (2012) 2366–2393. doi:10.1137/110856113.

[18] N. Guglielmi, C. Lubich, Low-rank dynamics for computing extremal points of real pseudospectra, SIAM. J. Matrix Anal. & Appl. 34 (1) (2013) 40–66. doi:10.1137/120862399.

[19] K. Meerbergen, W. Michiels, R. V. Beeumen, E. Mengi, Computation of pseudospectral abscissa for large-scale nonlinear eigenvalue problems, IMA J. Numer. Anal. (2017) drw065(In press). doi:10.1093/imanum/drw065.

[20] E. Mengi, E. A. Yildirim, M. Kiliç, Numerical optimization of eigenvalues of Hermitian matrix functions, SIAM. J. Matrix Anal. & Appl. 35 (2) (2014) 699–724. doi:10.1137/130933472.

[21] S. Gumussoy, M. L. Overton, Fixed-order $\mathcal{H}^\infty$ controller design via HIFOO, a specialized nonsmooth optimization package, in: Decision and Control, Institute of Electrical & Electronics Engineers (IEEE), 2008, pp. 4135–4140. doi:10.1109/acc.2008.4586909.

[22] J. Vanbiervliet, B. Vandereycken, W. Michiels, S. Vandewalle, M. Diehl, The smoothed spectral abscissa for robust stability optimization, SIAM J. Optim. 20 (1) (2009) 156–171. doi:10.1137/070704034.

[23] M. Diehl, K. Mombaur, D. Noll, Stability optimization of hybrid periodic systems via a smooth criterion, IEEE Trans. Autom. Control 54 (8) (2009) 1875–1880. doi:10.1109/tac.2009.2020669.

[24] K. Engelborghs, T. Luzyanina, D. Roose, Numerical bifurcation analysis of delay differential equations using DDE-BIFTOOL, ACM Trans. Math. Software 28 (1) (2002) 1–21. doi:10.1145/513001.513002.

[25] D. Xiu, G. E. Karniadakis, The wiener-askey polynomial chaos for stochastic differential equations, SIAM J. Sci. Comput. 24 (2) (2002) 619–644. doi:10.1137/s1064827501387826.

[26] R. Vermiglio, Polynomial chaos expansions for the stability analysis of uncertain delay differential equations (2016).

[27] W. Michiels, Spectrum-based stability analysis and stabilisation of systems described by delay differential algebraic equations, IET Control Theory A. 5 (16) (2011) 1829–1842. doi:10.1049/iet-cta.2010.0752.

[28] K. Schreiber, Nonlinear eigenvalue problems: Newton-type methods and nonlinear rayleigh functionals, Ph.D. thesis (2008).

[29] J. Dick, F. Y. Kuo, I. H. Sloan, High-dimensional integration: The quasi-Monte Carlo way, Acta Numerica 22 (2013) 133–288. doi:10.1017/s0962492913000044.

[30] W. J. Morokoff, R. E. Caflisch, Quasi-Monte Carlo integration, J. Comput. Phys. 122 (2) (1995) 218–230. doi:10.1006/jcph.1995.1209.

[31] R. E. Caflisch, Monte carlo and quasi-monte carlo methods, Acta Numerica 7 (1988) 1–49. doi:10.1017/S0962492900002804.

[32] D. Breda, S. Maset, R. Vermiglio, Pseudospectral differencing methods for characteristic roots of delay differential equations, SIAM J. Sci. Comput. 27 (2) (2005) 482–495. doi:10.1137/030601600.

[33] E. Talvila, Necessary and sufficient conditions for differentiating under the integral sign, Am. Math. Mon. 108 (6) (2001) 544–548. doi:10.2307/2695709.

[34] R. Hryniv, P. Lancaster, On the perturbation of analytic matrix functions, Integr. Equat. Oper. Th. 34 (3) (1999) 325–338. doi:10.1007/bf01300582.

[35] W. Michiels, I. Boussaada, S. I. Niculescu, An explicit formula for the splitting of multiple eigenvalues for nonlinear eigenvalue problems, and connections with the linearization for the delay eigenvalue problem, SIAM. J. Matrix Anal. & Appl.(In review).

[36] L. Fenzi, W. Michiels, A matlab tool for the optimization of uncertain delay differential equations (uddae_optimization) (2016).
URL http://twr.cs.kuleuven.be/research/software/delay-control/UDDAE_optimization/

[37] T. Vyhlídal, P. Zítek, K. Paulů, Design, modelling and control of the experimental heat transfer set-up, in: Topics in Time Delay Systems, Springer-Verlag, Berlin Heidelberg, 2009, pp. 303–313. doi:10.1007/978-3-642-02897-7_26.

[38] W. Michiels, T. Vyhlídal, P. Zítek, Control design for time-delay systems based on quasi-direct pole placement, J. Process Control 20 (3) (2010) 337–343. doi:10.1016/j.jprocont.2009.11.004.